International Journal of Applied Power Engineering (IJAPE)
Vol. 11, No. 3, September 2022, pp. 218~228
ISSN: 2252-8792, DOI: 10.11591/ijape.v11.i3.pp218-228

Hybrid MPPT-based predictive speed control model for variable speed PMSG wind energy conversion systems

Mai N. Abu Hashish, Ahmed Ali Daoud, Medhat Hegazy Elfar
Department of Electrical Power Engineering, Port-Said University, Port-Said, Egypt

Article Info

Article history:

Received Mar 3, 2021
Revised Aug 1, 2022
Accepted Aug 9, 2022

Keywords:

MPC
MPPT
PMSG
WECS

ABSTRACT

In this research, a predictive speed control (PSC) technique based on permanent magnet synchronous generators is proposed for variable-speed wind energy conversion systems (VS-WECS) (PMSG). The control approach that has been developed makes it possible to regulate mechanical and electrical variables concurrently within the context of a single cost function. The power converter will then use the optimum switching state that will result in the lowest possible cost function when it has been chosen. The maximum power point tracking (MPPT) algorithms used in the proposed control approach are combined in order to achieve optimum efficiency. As a direct result of this, the conventional cascade structure of proportional-integral (PI) controllers has been removed, which results in an improvement in the system's dynamic responsiveness. In addition, predictive current control, also known as PCC, is implemented on the grid-side converter, also known as the GSC, in order to accomplish decoupled grid current control. Using MATLAB/SIMULINK, we analyze the performance of the suggested control methods and compare it to the performance of a traditional PI speed controller. The findings demonstrated that the MPC controller is superior than the PI controller in terms of its ability to handle system dynamics.

Corresponding Author:

Ahmed Ali Daoud
Department of Electrical Power Engineering, Port Said University
Port Fouad, Port Said, 42523, Egypt
Email: a.daoud@psu.edu.eg, ahmed.ali.daoud@gmail.com

1. INTRODUCTION

With the growing demand for electrical energy, an increasing attention was paid to search for alternative methods of electricity generation. Renewable energy sources are considered as the best alternative methods of electricity generation compared to the conventional ones. This is mainly due to that the conventional sources of energy have several drawbacks, such as relying on burning fossil fuels, which has a bad side effect on the Earth's atmosphere and the non-renewable nature of fossil fuels. Renewable energy is an abundant and clean energy, which has been considered as an effective solution to overcome the aforementioned problems. Wind power is recognized as one of the renewable energy sources that is expanding at one of the highest rates [1]. Wind power is only one of various forms of renewable energy sources. In many countries, the integration of wind power production into the utility grid has developed into an integral component of the process. According to [2], the global market for wind power capacity increased by around 60 GW in 2019.

Wind generators and power converters are the two primary electrical components that make up wind energy conversion systems (WECS). Different kinds of WECS have been created as a result of the worldwide wind power markets by combining these two components in a wide variety of permutations and combinations. These may be broken down into WECS with a constant speed, also known as FS-WECS, and

WECS with a variable speed, known as VS-WECS [3]–[5]. The efficiency of wind energy conversion is greatest in type 4 WECS [3] out of all of these kinds of wind energy conversion systems. Therefore, the type 4 WECS has the benefit of being able to achieve fully variable-speed operation; hence, it is feasible to acquire the maximum potential power at a variety of various wind speeds [6]. The permanent magnet synchronous generator, also known as a PMSG, is the most popular option for use in type 4 WECS because it features direct-drive operation, eliminates the requirement for a DC excitation system, reduces rotor losses, and requires less maintenance than other types of generators [7].

In vertical-axis wind energy conversion systems (VS-WECS), it is essential to get the greatest possible amount of power from the wind in order to achieve the highest possible degree of energy conversion efficiency. This is because of the unpredictable nature of the wind. There is an essential design parameter for wind turbines (WT) called the optimal tip speed ratio (TSR), which ensures that the amount of electricity that is harnessed is increased to its full potential. In order to maintain the ideal TSR at all times, variable-speed wind turbines, also known as VSWTs, are able to modify the rotating speed of their blades in response to instantaneous shifts in the wind speed [8]. It is very necessary to have a maximum power point tracking (MPPT) algorithm in order to collect the most possible power from the wind. The optimal TSR and optimal torque (OT) control methods are widely used in WT systems. These methods provide the best compromise between complexity and performance across a wide range of wind speeds [4], [7]–[12]. Among the various MPPT control techniques that have been applied to wind energy systems, the optimal TSR and optimal torque (OT) control methods are the most common.

Power electronic converters are essential components in WECS because they allow the system to function in variable-speed conditions and make it possible for wind turbines to connect to the grid [13]. These converters take the variable voltage and frequency produced by the wind generator and convert it into a fixed voltage and frequency. Back-to-back (BTB) connected converters, which are similar on both the machine-side and grid-side and are coupled by a DC-link capacitor, are often used in type 4 WECS [14]. Back-to-back converters are denoted by the acronym "BTB."

Several control systems for precise control to accomplish the intended operation and boost WECS energy conversion efficiency have been developed. Traditional control approaches, such as linear control using pulse width modulation (PWM) and nonlinear hysteresis control, are extensively documented in the literature and commonly used to regulate machine-side converters (MSC) and grid-side converters (GSC) in WT systems [6], [15]–[17]. The most commonly used linear control methods for MSCs and GSCs, respectively, are field oriented control (FOC) and voltage-oriented control (VOC), in which a cascaded configuration of proportional-integral (PI) controllers is used in the outer and inner control loops and the PWM stage to generate the switching signals for the power converters [12], [14], [18], [19]. The FOC scheme for MSC in type 4 WECS with PMSG has a fast inner current control loop implemented in synchronously rotating dq-axes reference frame to obtain decoupled control of generator currents, combined with an outer slower speed control loop for regulating the generator speed at its reference value. Meanwhile, the VOC design for GSC includes an outside DC-link voltage management loop to keep the DC-link voltage constant and an inner current loop to inject actual power from the MSC to the grid at unity power factor [20], [21]. Nonetheless, traditional linear control approaches have several limitations. The linear controller's transient response is heavily influenced by the setting of various gain levels in the PI cascaded control structure. Control variables such as dq-axes generators or grid currents display significant coupling effects; hence, extra feed-forward terms are required for decoupling of dq components of the current with increased control complexity. The nature of the control variables influences steady-state performance, which is best in the dq-axes reference frame. Others may be found in [13], [22]–[24] for modest dynamic performance. Because of the rapid advancement of microprocessors, it is now feasible to use more complicated control methods to increase energy conversion efficiency and achieve optimum system performance.

One of these sophisticated control methods, model predictive control (MPC), has numerous significant features that make it appropriate for power converter control [13], [25]–[28]. According to the literature, MPC is simple to grasp and can be used to a wide range of systems. When compared to linear controllers, MPC may give an outstanding transient response. There are two kinds of MPC schemes: continuous-control-set MPC (CCS-MPC) and finite-control-set MPC (FCS-MPC) [25], [26]. The controller output in CCS-MPC systems is a continuous reference signal that requires a modulator to create switching signals. FCS-MPC, on the other hand, takes use of the power converters' limited number of switching states, and a discrete-time (DT) model of the system is utilized to forecast the behavior of the variables just for those potential switching states. The projected values of the variables are then utilized to calculate a cost function, and the switching state that minimizes the cost function is chosen and applied directly to the converter [23], [26], [27]. As a result, in type 4 WECS, FCS-MPC leveraged the operational principles of the FOC scheme to create predictive current control (PCC) for PMSG by merely changing the inner PI current control loops, which increases the control system's dynamic responsiveness [4], [10], [29], [30]. However, a cascaded structure with a PI speed controller is still used, and the dynamic responsiveness of the outer speed loop may be increased. In [21], an MPC method is implemented just for MSC in PMSG VS-WECS as a substitute for the PI speed controller in the outer loop, with the inner loop employed for current control using a traditional hysteresis controller. As a result, cascaded control configuration remains in the MSC control scheme. MPC enables the incorporation of several variables into a single cost function without the need for a cascaded structure or an external PI speed control loop. In [26], [31]–[35], the predictive speed control (PSC) approach was applied to a permanent magnet synchronous motor (PMSM), allowing simultaneous modification of the speed and electrical variables in a single control law. In [36], a PSC scheme for PMSG in WT systems is given; however, the control method implementation does not take into consideration the WT system's features.

In this study, a PSC approach for PMSG VS-WECS is presented for further investigation. To locate the ideal switching state of the power converter without the use of a cascade structure, the mechanical speed as well as the electrical variables (i.e., speed and current/torque) are included into a single cost function. The solution that has been suggested is straightforward and takes into consideration the fundamental workings of WT systems. A comparison is made between the efficiency of the suggested PSC technique and that of the conventional approach (i.e., PI speed controller in the outer loop and PCC in the inner current control loop). The PCC scheme, on the other hand, is implemented on the GSC in order to inject actual power into the grid while maintaining a power factor of unity. The following is a condensed version of the primary contributions that this paper makes: i) Elimination of the well-known cascaded structure of PI controllers for the MSC in PMSG VS-WECS by controlling mechanical and electrical variables in a single control loop with the PSC scheme; ii) The proposed control method is based on a combination of two MPPT algorithms, namely optimal TSR and OT control; iii) Because the control variables have different natures, error terms, including normalization, have been added to the cost function; iv) A comparison of the proposed PSC method and the traditional one is carried out under wind speed variation (i.e., PI speed controller in the outer loop and PCC in the inner current control loop); v) PCC is also applied to the GSC as a replacement for the inner PI current control loop; and vi) The effectiveness of the proposed control methods is evaluated using MATLAB simulations.

This paper is organized as follows: section 2 presents the model of type 4 WECS with PMSG. The MPPT algorithms are discussed in section 3. The FCS-MPC principles and the proposed speed and current control strategies are described in section 4. The performance of the system is tested via simulations in section 5. Finally, the conclusion of this work is given in section 6.

2. MODELING OF TYPE 4 WECS WITH PMSG

Figure 1 depicts the system setup of a type 4 VS-WECS equipped with PMSG. It is a three-phase PMSG that is directly linked to the WT and constitutes this component. Through the attached two-level voltage source converter of BTB, the stator of PMSG is in electrical communication with the grid (2L-VSC). The MSC and GSC are connected to one another by a DC-link capacitor, which prevents the generator and the grid from being connected to one another.

2.1. Wind turbine model

Wind turbines transform the kinetic energy of the wind into mechanical energy, which is then used to drive the generator rotor and produce electrical energy. The output of the wind power in the form of mechanical power is provided by [37]:

$$P_m = \frac{1}{2}\rho A C_p(\lambda, \beta) V_w^3 \tag{1}$$

where ρ is the air density (kg/m^3), A is area swept by the WT blades (m^2), V_w is the wind speed (m/s), C_p is the power coefficient of the WT which is a function of TSR (λ) and blade pitch angle (β). The TSR is an important parameter of the WT expressing the ratio of the blade tip speed to the incoming wind speed, and can be defined by (2):

$$\lambda = \frac{\omega_m R}{V_w} \tag{2}$$

where ω_m is the rotational speed of turbine rotor (rad/s) and R is the length of the blade (m). In this paper, the value of C_p can be determined from (3) and (4):

$$C_p(\lambda, \beta) = C_1\left(\frac{C_2}{\lambda_i} - C_3\beta - C_4\right)e^{\frac{-C_5}{\lambda_i}} + C_6\lambda \tag{3}$$

$$\frac{1}{\lambda_i} = \frac{1}{\lambda+0.08\beta} - \frac{0.035}{1+\beta^3} \tag{4}$$

where the turbine coefficients $C_1 - C_6$ are given as: $C_1 = 0.5176, C_2 = 116, C_3 = 0.4, C_4 = 5, C_5 = 21, C_6 = 0.0068$ [16]. The mechanical torque developed by a WT is given by:

$$T_m = \frac{P_m}{\omega_m} \tag{5}$$

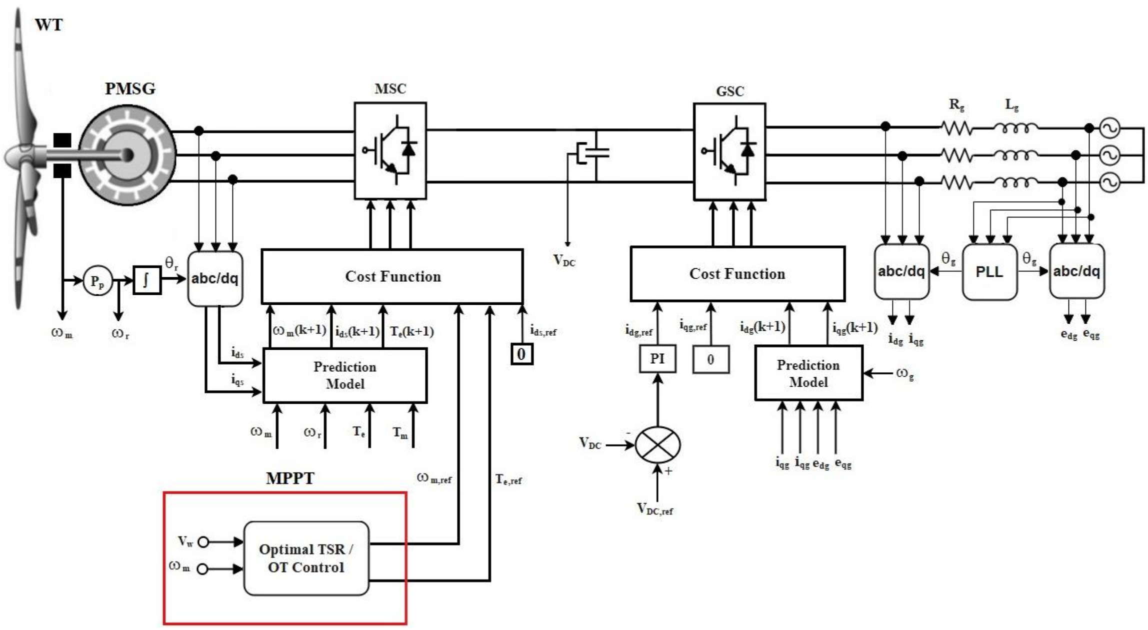

Figure 1. Grid-connected PMSG based wind energy conversion system

2.2. PMSG dynamic model

Depending on the amount of shaft mechanical torque applied, a permanent magnet synchronous machine, also known as a PMS machine, may either function as a motor or a generator (T_m). The flow of the current and the direction of the power are both altered, yet the dynamics of the machine are unaffected. In applications using wind energy, the PMS machine functions as a generator by only reversing the sign of the mechanical torque [13]. In the *dq* reference frame, the equations for the stator voltage of the three-phase PMSG may be written as [29]:

$$v_{ds} = R_s i_{ds} + L_d \frac{d}{dt} i_{ds} - \omega_r L_q i_{qs} \tag{6}$$

$$v_{qs} = R_s i_{qs} + L_q \frac{d}{dt} i_{qs} + \omega_r L_d i_{ds} + \omega_r \psi_r \tag{7}$$

where i_{ds} and i_{qs} are the *dq*-axes stator currents, R_s is the stator winding resistance, L_d and L_q are the *dq*-axes stator inductances, ω_r is the electrical angular speed of the generator, ψ_r is the permanent magnet flux linkage. The electromagnetic torque T_e of the PMSG is given by:

$$T_e = \frac{3}{2} P_p \left[\psi_r i_{qs} + \left(L_d - L_q\right) i_{ds} i_{qs}\right] \tag{8}$$

where P_p is the pole pairs number. In surface-mounted PMSG (SPMSG), L_d and L_q are equal; i.e., $L_d = L_q = L_s$. Hence, the electromagnetic torque in (8) can be rewritten as:

$$T_e = \frac{3}{2} P_p \psi_r i_{qs} \tag{9}$$

The mechanical equation of rotor speed dynamics is given by:

$$J\frac{d}{dt}\omega_m + F\omega_m = T_e - T_m \quad (10)$$

where ω_m is the mechanical angular speed of the generator. J is the moment of inertia ($kg.m^2$) and F is the friction coefficient ($N.m.s$). The relation between mechanical and electrical angular speed is given by:

$$\omega_r = P_p\omega_m \quad (11)$$

According to (10), the control of the rotational speed of the generator may be accomplished by adjusting the amount of electromagnetic torque that is applied. In addition, according to (9), since the permanent magnet flux linkage ψ_r of PMSG has a constant value, the electromagnetic torque can be controlled by controlling the q-axis component of stator current only. As a result, the generator speed control is accomplished by modifying the q-axis stator current component of PMSG. A zero value is assigned to the stator d-axis current component in order to maximize the efficiency of the machine by reducing the amount of stator current that flows for a given torque [16], [30].

3. MPPT ALGORITHMS

The operating regions of wind turbines can be divided into four different regions as shown in Figure 2. Below cut-in wind speed (region 1), WTs are kept in parking mode, where the wind power is negligible and insufficient to overcome the inertia of the WTs. Above cut-out wind speed (region 4), WTs are shut down to ensure safety. In region 3, for wind speed values between rated and cut-out, the pitch controller is employed to reduce mechanical stress on the WT, and turbine power is limited to its rated value to protect the WT and generator from being overloaded. Finally, the mechanical power maintains a cubic relationship with wind speed in region 2, which is bounded by the cut-in and rated speed [8]. MPPT is activated in this region and the turbine produces the maximum possible power from the wind. This paper focuses on region 2, where the MPPT technique is needed. In VS-WECS, the MPPT control scheme is applied to extract maximum available power during varying wind speed conditions. Figure 3 shows C_p as a function of λ at pitch angle β equals zero. Continuous operation of the WT at λ_{opt}, where C_p is maximum, guarantees that the extracted power will be maximized at any wind speed [8]. The optimal TSR and OT control methods are applied in this work.

The optimal TSR control provides generator reference speed (12) by adjusting generator speed in proportion to varying wind speed conditions, such that the WT always tracks maximum power points (MPP) and operates at maximum C_p and optimal TSR λ_{opt} as illustrated in Figure 4 [9].

$$\omega_{m,ref} = \frac{\lambda_{opt}V_w}{R} = K_1^{opt}V_w \quad (12)$$

In case of OT MPPT method, the expression for the reference electromagnetic torque $T_{e,ref}$ can be written as a function of the measured mechanical generator speed ω_m and WT parameters [7], [13]:

$$T_{e,ref} = \frac{1}{2}\rho\pi R^5\frac{C_{p-max}}{\lambda_{opt}^3}\omega_m^2 = K_2^{opt}\omega_m^2 \quad (13)$$

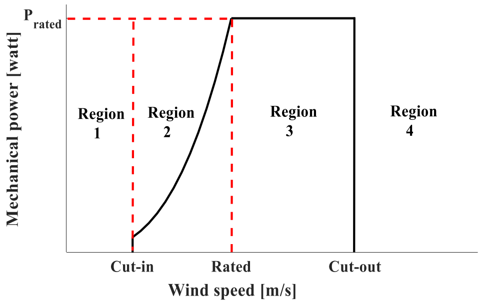

Figure 2. Wind turbine operating regions

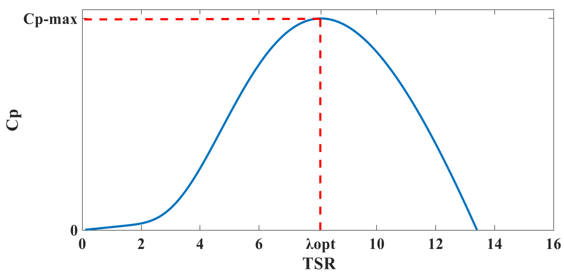

Figure 3. Power coefficient vs tip speed ratio

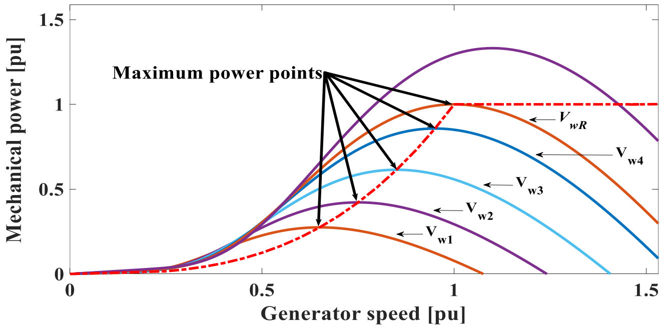

Figure 4. Power characteristic of wind turbine

4. FINITE-CONTROL-SET MODEL PREDICTIVE CONTROL

The FCS-MPC control technique is based on the facts that a power converter can only create a limited number of switching states and that the future behavior of the variables may be predicted by using a discrete model of the system for each switching state. The use of a cost function determines the projected values, which in turn determines which switching state should be chosen. It is not necessary to include a modulation stage in order to choose and create for the power converter the switching state that would result in the lowest value for this cost function [26], [27]. In this study, the FCS-MPC method is used to adjust generator speed to its optimum value at various wind speeds measured at MSC. In addition to this, it may be used to manage grid currents by acting as a substitute for the inner PI current control loop at GSC. On the other hand, the outer loop is put to use to regulate DC-link voltage by means of a PI controller.

4.1. Proposed predictive speed control for MSC

The planned power supply cabinet (PSC) at MSC is shown in diagram form in Figure 1. In order to arrive at the predictive model for the purpose of designing the PSC scheme, the continuous-time (CT) model of SPMSG will need to be discretized. This model is used in order to make predictions about the future behavior of the system variables at the subsequent sampling moment. Using (6) and (7), we can determine how the current through the *dq* frame stator varies as a function of time in SPMSG.

$$\frac{d}{dt}i_{ds} = -\frac{R_s}{L_s}i_{ds} + \omega_r i_{qs} + \frac{1}{L_s}v_{ds} \tag{14}$$

$$\frac{d}{dt}i_{qs} = -\frac{R_s}{L_s}i_{qs} - \omega_r i_{ds} + \frac{1}{L_s}v_{qs} - \frac{\omega_r\psi_r}{L_s} \tag{15}$$

By using the forward Euler approximation method, the first order derivatives of generator mechanical speed and the stator currents in (10), (14), and (15) can be discretized with sampling time T_s as:

$$\frac{dx}{dt} = \frac{x(k+1)-x(k)}{T_s} \tag{16}$$

Hence, the DT model of stator current and generator mechanical speed of SPMSG can be written as:

$$i_{ds}(k+1) = \left(1-\frac{R_sT_s}{L_s}\right)i_{ds}(k) + \omega_r(k)T_s i_{qs}(k) + \frac{T_s}{L_s}v_{ds}(k) \tag{17}$$

$$i_{qs}(k+1) = \left(1-\frac{R_sT_s}{L_s}\right)i_{qs}(k) - \omega_r(k)T_s i_{ds}(k) + \frac{T_s}{L_s}v_{qs}(k) - \frac{\omega_r(k)\psi_r T_s}{L_s} \tag{18}$$

$$\omega_m(k+1) = \omega_m(k) + \frac{T_s}{J}\big(T_e(k+1) - T_m(k)\big) \tag{19}$$

A single cost function, g_M, is used in the PSC plan that has been suggested, and it takes into account both mechanical and electrical factors. As a result, the structure of the cascading loop has been done away with. The cost function might be constructed as follows:

$$g_M = g_1 + g_2 + g_3 + g_c \tag{20}$$

where:

$$g_1 = \frac{|\omega_{m,ref} - \omega_m(k+1)|}{\omega_{m,rated}} \tag{21}$$

$$g_2 = \frac{|i_{ds,ref} - i_{ds}(k+1)|}{I_s} \tag{22}$$

$$g_3 = \frac{|T_{e,ref} - T_e(k+1)|}{T_{e,rated}} \tag{23}$$

$$g_c = \begin{cases} \infty, if \sqrt{i_{ds}(k+1)^2 + i_{qs}(k+1)^2} > I_s \\ 0, otherwise \end{cases} + \begin{cases} \infty, if\ \omega_m > \omega_{m,rated} \\ 0, otherwise \end{cases} \tag{24}$$

The first term, which is produced from the most effective TSR MPPT method, is utilized to monitor the mechanical reference speed. The second term is known as the d-axis stator current term, and it is implemented in the SPMSG in order to accomplish a zero direct axis current control approach (i.e., $i_{ds,\ ref}$=0). The third term ensures that the electromagnetic torque stays at the value that was determined by the OT algorithm as the reference value. Therefore, in steady state, T_e is equal to T_m, and the final term is a restricted term, which means that it equals zero while circumstances are normal but may equal infinite if the stator current amplitude or speed is greater than their rated values (i.e., I_s or $\omega_{m,\ rated}$). It is not possible to choose the voltage vectors that are responsible for such very high function cost values.

It is possible to compute the future values of *dq* stator currents and generator mechanical speed by using the predictive model presented in (17), (18), and (19). The seven alternative switching state combinations that are available with 2L-VSC each result in one of seven different values for and. In turn, these values result in seven distinct values for i_{ds} (k+1), i_{qs} (k+1), and ω_m (k+1). In the end, the predicted variables are assessed, and the switching state that has a cost function that is the lowest is selected as the optimum action to apply to MSC [13], [38].

4.2. Predictive current control for GSC

Figure 1 demonstrates how the PCC approach may be used to GSC in order to manage the active and reactive power that is injected into the grid. The following are the voltages for the *dq*-axes of the GSC:

$$v_{dg} = R_g i_{dg} + L_g \frac{d}{dt} i_{dg} - \omega_g L_g i_{qg} + e_{dg} \tag{25}$$

$$v_{qg} = R_g i_{qg} + L_g \frac{d}{dt} i_{qg} + \omega_g L_g i_{dg} + e_{qg} \tag{26}$$

where i_{dg} and i_{qg} are the *dq* grid currents, ω_g is the grid angular frequency, L_g and R_g are the grid filter inductance and resistance, respectively, e_{dg} and e_{qg} are the *dq* grid voltages. By using the forward Euler approximation method, the DT model of grid currents is given as:

$$i_{dg}(k+1) = \left(1 - \frac{R_g T_s}{L_g}\right) i_{dg}(k) + \omega_g T_s i_{qg}(k) + \frac{T_s}{L_g}\left(v_{dg}(k) - e_{dg}(k)\right) \tag{27}$$

$$i_{qg}(k+1) = \left(1 - \frac{R_g T_s}{L_g}\right) i_{qg}(k) - \omega_g T_s i_{dg}(k) + \frac{T_s}{L_g}\left(v_{qg}(k) - e_{qg}(k)\right) \tag{28}$$

The cost function for GSC is designed as:

$$\begin{aligned} g_G &= |i_{dg,ref} - i_{dg}(k+1)| + |i_{qg,ref} - i_{qg}(k+1)| \\ &\quad + \begin{cases} \infty, if \sqrt{i_{dg}(k+1)^2 + i_{qg}(k+1)^2} > I_g \\ 0, otherwise \end{cases} \end{aligned} \tag{29}$$

with a constrained term, which penalizes the voltage vectors that cause grid current exceeding its rated value (i.e., I_g). The reference value of *d*-axis grid current $i_{dg,\ ref}$ is obtained from an outer DC-link voltage PI control loop, while the reference value of *q*-axis grid current $i_{qg,\ ref}$ is set to zero to inject pure active power to the grid. Again, the seven possible switching state combinations of 2L-VSC give seven different values for v_{dg}

and v_{qg}, which in turn, leads to seven different values for i_{dg} $(k+1)$ and i_{qg} $(k+1)$. The predicted grid currents are then evaluated using the cost function in (29) and the switching state that minimizes the current error is selected as an optimal action and applied to GSC.

5. SIMULATION RESULTS

The performance of the proposed control schemes applied to PMSG VS-WECS is studied and evaluated through a simulation model built in MATLAB/Simulink. The system parameters are listed in Table 1. To investigate the dynamic performance of the proposed PSC strategy and classical one for MSC control, a step change in wind speed profile is assumed as shown in Figure 5. By comparing Figures 5(a) and 5(b), it is seen that below rated wind speed, the C_p and the TSR are at their optimal values (C_p=0.48 and λ_{opt}=8.11); however, the proposed control method gives a better performance than that of the classical one.

Table 1. System parameters

Parameter	Symbol	Value	Parameter	Symbol	Value
Blade radius	R	1.6 m	Moment of inertia	J	0.01 $Kg.m^2$
Optimal tip speed ratio	λ_{opt}	8.1	Permanent magnet flux linkage	ψ_r	0.85 Wb
Maximum power coefficient	C_p	0.48	DC-link voltage	V_{dc}	700 V
Rated wind speed	V_w	20 m/s	Capacitor of the DC-link	C	3 mF
PMSG RMS line voltage	V_s	400 V	Grid frequency	f	50 Hz
Pole pairs number	P_p	3	Grid resistance	R_g	0.16 Ω
Stator resistance	R_s	0.2 Ω	Grid inductance	L_g	10 mH
Stator inductance	L_s	15 mH			

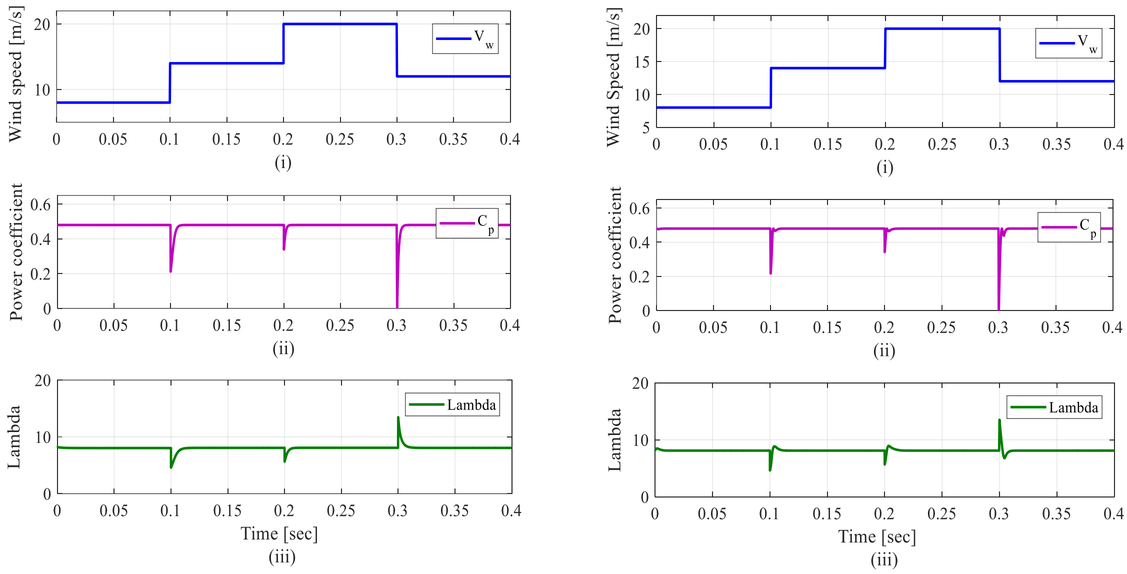

(a) (b)

Figure 5. The characteristics of WT (a) proposed PSC method and (b) classical speed control method

Figures 6(a) and 6(b) illustrate the capability of the speed controllers to regulate the mechanical speed of the generator in accordance with its reference value (b). In Figures 6(a) and 6(b), Figure (i) which ensures that the maximum amount of power is extracted despite changes in wind speed, is shown. When the proposed PSC is used to control the speed of the mechanical rotor, it is noted that there is no overshoot in the speed of the rotor, in contrast to the traditional PI speed controller. In addition, the proposed technique results in a settling time of 6.8 milliseconds (within a 5% tolerance band), whereas the PI controller results in a settling time of 11.2 milliseconds. As can be seen in Figures 6(a) and 6(b), the electromagnetic torque follows the mechanical torque in a manner that is entirely accurate (ii). However, when compared to the traditional control method, the dynamic response of Te when utilizing the new control method is much improved. The dynamic response of the phase-a stator current and the dq stator current components is illustrated in Figure 6(a) and 6(b) (iii), respectively.

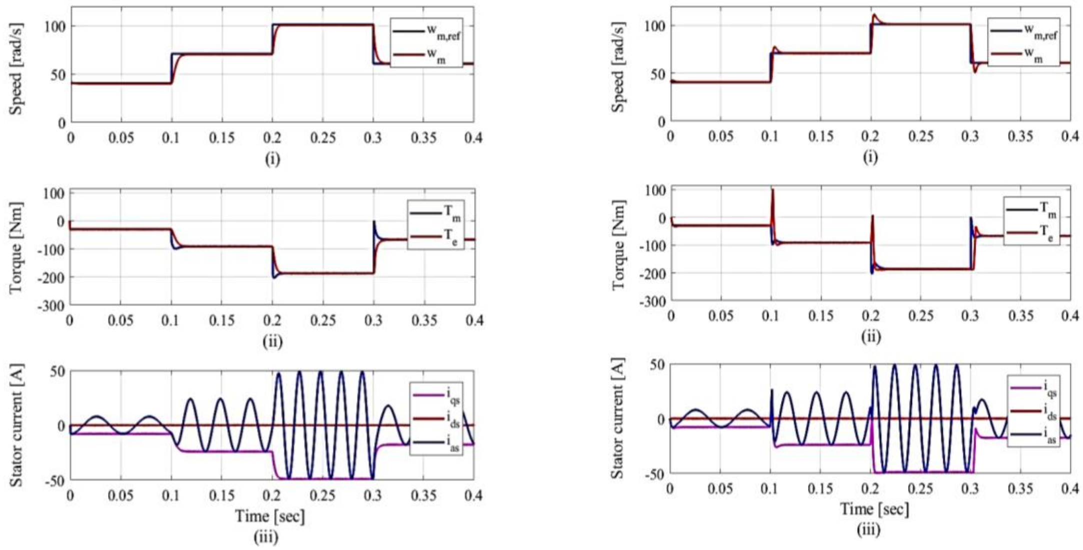

(a) (b)

Figure 6. Generator side control results (a) proposed PSC method and (b) classical speed control method

Using the proposed PSC approach, the magnitude and frequency of phase-a stator current vary smoothly with generator mechanical speed. The *d*-axis stator current remains constant, whereas the *q*-axis stator current varies linearly with T_e. We also notice that the regulation of the stator current's dq components is significantly disconnected. Figure 7 depicts the GSC control results, on the other hand. As seen in Figure 7, the DC-link voltage follows its reference value (i). Figures 7(ii) and 7(iii) illustrate that the d-axis grid current follows the active power with the change in wind speed, while the q-axis current is driven to zero to inject zero reactive power into the grid. The grid voltage and current are in phase, resulting in unity power factor functioning, as illustrated in Figure 7(iv).

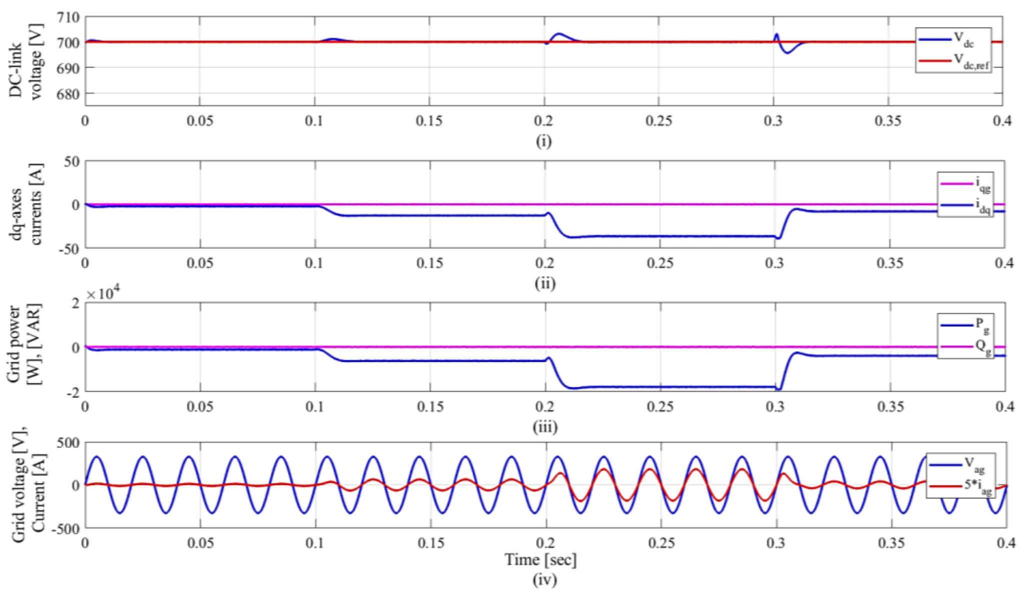

Figure 7. Grid side control results

6. CONCLUSION

In this research, a predictive speed control (PSC) method is given for the model predictive control (MPC) in the PMSG VS-WECS. The PSC strategy is based on the operational principles of a finite-control-set model predictive control (FCS-MPC). Controlling both the mechanical and electrical variables inside a single cost function allows the proposed control technique to avoid the requirement for the cascaded control structure. This allows the control method to create the optimal switching signal for the power converter. The maximum power point tracking (MPPT) algorithms used in the proposed control approach are combined in order to achieve maximum efficiency. In addition, a predictive current control, also known as PCC, is implemented in place of a PI current control loop within the GSC in order to maintain control over the active and reactive power that is injected into the grid. Through the use of MATLAB simulations, we evaluate how well the system functions when subjected to varying wind speeds. The simulation results demonstrated that MPC is superior to classic PI controllers whenever there is a change in the speed of the wind.

REFERENCES

[1] N. Huang, "Simulation of power control of a wind turbine permanent magnet synchronous generator system," M.S. thesis, Department of Electrical and Computer Engineering, Marquette University, Milwaukee, USA, 2013.

[2] Global Wind Energy Council, "Global wind report 2019," *Global Wind Energy Council (GWEC)*, 2019. https://gwec.net/global-wind-report-2019/.

[3] V. Yaramasu, B. Wu, P. C. Sen, S. Kouro, and M. Narimani, "High-power wind energy conversion systems: state-of-the-art and emerging technologies," *Proceedings of the IEEE*, vol. 103, no. 5, pp. 740–788, May 2015, doi: 10.1109/JPROC.2014.2378692.

[4] V. Yaramasu, S. Kouro, A. Dekka, S. Alepuz, J. Rodriguez, and M. Duran, "Power conversion and predictive control of wind energy conversion systems," in *Advanced Control and Optimization Paradigms for Wind Energy Systems*, R.-E. Precup, T. Kamal, and S. Z. Hassan, Eds. Singapore: Springer, 2019, pp. 113–139, doi: 10.1007/978-981-13-5995-8_5.

[5] V. Yaramasu and B. Wu, "Power electronics for high-power wind energy conversion systems," in *Encyclopedia of Sustainable Technologies*, Amsterdam: Elsevier, 2017, pp. 37–49.

[6] Y. Errami, M. Ouassaid, and M. Maaroufi, "Control of a PMSG based wind energy generation system for power maximization and grid fault conditions," *Energy Procedia*, vol. 42, pp. 220–229, 2013, doi: 10.1016/j.egypro.2013.11.022.

[7] V. Yaramasu, A. Dekka, M. J. Durán, S. Kouro, and B. Wu, "PMSG-based wind energy conversion systems: survey on power converters and controls," *IET Electric Power Applications*, vol. 11, no. 6, pp. 956–968, Jul. 2017, doi: 10.1049/iet-epa.2016.0799.

[8] M. A. Abdullah, A. H. M. Yatim, C. W. Tan, and R. Saidur, "A review of maximum power point tracking algorithms for wind energy systems," *Renewable and Sustainable Energy Reviews*, vol. 16, no. 5, pp. 3220–3227, Jun. 2012, doi: 10.1016/j.rser.2012.02.016.

[9] D. Kumar and K. Chatterjee, "A review of conventional and advanced MPPT algorithms for wind energy systems," *Renewable and Sustainable Energy Reviews*, vol. 55, pp. 957–970, Mar. 2016, doi: 10.1016/j.rser.2015.11.013.

[10] M. Abdelrahem, C. Hackl, and R. Kennel, "Model predictive control of permanent magnet synchronous generators in variable-speed wind turbine systems," *Proceedings of Power and Energy Student Summit (PESS 2016)*, 2016.

[11] H. H. H. Mousa, A.-R. Youssef, and E. E. M. Mohamed, "Model predictive speed control of five-phase PMSG based variable speed wind generation system," in *2018 Twentieth International Middle East Power Systems Conference (MEPCON)*, Dec. 2018, pp. 304–309, doi: 10.1109/MEPCON.2018.8635190.

[12] D. K. Porate, S. P. Gawande, A. P. Munshi, K. B. Porate, S. G. Kadwane, and M. A. Waghmare, "Zero direct-axis current (ZDC) control for variable speed wind energy conversion system using PMSG," *Energy Procedia*, vol. 117, pp. 943–950, Jun. 2017, doi: 10.1016/j.egypro.2017.05.214.

[13] V. Yaramasu and B. Wu, *Model predictive control of wind energy conversion systems*. Hoboken, NJ, USA: John Wiley & Sons, 2016.

[14] K. Milev, V. Yaramasu, A. Dekka, and S. Kouro, "Modulated predictive current control of PMSG-based wind energy systems," in *2020 11th Power Electronics, Drive Systems, and Technologies Conference (PEDSTC)*, Feb. 2020, pp. 1–6, doi: 10.1109/PEDSTC49159.2020.9088365.

[15] S. M. Tripathi, A. N. Tiwari, and D. Singh, "Optimum design of proportional-integral controllers in grid-integrated PMSG-based wind energy conversion system," *International Transactions on Electrical Energy Systems*, vol. 26, no. 5, pp. 1006–1031, May 2016, doi: 10.1002/etep.2120.

[16] A. H. Kasem Alaboudy, A. A. Daoud, S. S. Desouky, and A. A. Salem, "Converter controls and flicker study of PMSG-based grid connected wind turbines," *Ain Shams Engineering Journal*, vol. 4, no. 1, pp. 75–91, Mar. 2013, doi: 10.1016/j.asej.2012.06.002.

[17] A.-R. Youssef, M. A. Sayed, and M. Abdel-Wahab, "MPPT control technique for direct-drive five-phase pmsg wind turbines with wind speed estimation," *variations*, vol. 21, p. 22, 2015.

[18] M. Abdelrahem, C. Hackl, Z. Zhang, and R. Kennel, "Sensorless control of permanent magnet synchronous generators in variable-speed wind turbine systems," *Proceedings of Power and Energy Student Summit (PESS 2016)*, 2016.

[19] M. Abdelrahem, C. M. Hackl, and R. Kennel, "Implementation and experimental investigation of a sensorless field-oriented control scheme for permanent-magnet synchronous generators," *Electrical Engineering*, vol. 100, no. 2, pp. 849–856, Jun. 2018, doi: 10.1007/s00202-017-0554-y.

[20] S. Li, T. A. Haskew, and L. Xu, "Conventional and novel control designs for direct driven PMSG wind turbines," *Electric Power Systems Research*, vol. 80, no. 3, pp. 328–338, Mar. 2010, doi: 10.1016/j.epsr.2009.09.016.

[21] H. H. H. Mousa, A. Youssef, and E. E. M. Mohamed, "Model predictive speed control of five-phase permanent magnet synchronous generator-based wind generation system via wind-speed estimation," *International Transactions on Electrical Energy Systems*, vol. 29, no. 5, p. e2826, May 2019, doi: 10.1002/2050-7038.2826.

[22] J. Rodriguez *et al.*, "Predictive current control of a voltage source inverter," *IEEE Transactions on Industrial Electronics*, vol. 54, no. 1, pp. 495–503, Feb. 2007, doi: 10.1109/TIE.2006.888802.

[23] H. A. Young, M. A. Perez, J. Rodriguez, and H. Abu-Rub, "Assessing finite-control-set model predictive control: a comparison with a linear current controller in two-level voltage source inverters," *IEEE Industrial Electronics Magazine*, vol. 8, no. 1, pp. 44–52, Mar. 2014, doi: 10.1109/MIE.2013.2294870.

[24] J. Rodriguez and P. Cortes, *Predictive control of power converters and electrical drives*. Hoboken, NJ, USA: John Wiley & Sons, 2012.

[25] P. Cortes, M. P. Kazmierkowski, R. M. Kennel, D. E. Quevedo, and J. Rodriguez, "Predictive control in power electronics and drives," *IEEE Transactions on Industrial Electronics*, vol. 55, no. 12, pp. 4312–4324, Dec. 2008, doi: 10.1109/TIE.2008.2007480.

[26] J. Rodriguez *et al.*, "State of the art of finite control set model predictive control in power electronics," *IEEE Transactions on Industrial Informatics*, vol. 9, no. 2, pp. 1003–1016, May 2013, doi: 10.1109/TII.2012.2221469.

[27] S. Kouro, P. Cortes, R. Vargas, U. Ammann, and J. Rodriguez, "Model predictive control—a simple and powerful method to control power converters," *IEEE Transactions on Industrial Electronics*, vol. 56, no. 6, pp. 1826–1838, Jun. 2009, doi: 10.1109/TIE.2008.2008349.
[28] S. Vazquez, J. Rodriguez, M. Rivera, L. G. Franquelo, and M. Norambuena, "Model predictive control for power converters and drives: advances and trends," *IEEE Transactions on Industrial Electronics*, vol. 64, no. 2, pp. 935–947, Feb. 2017, doi: 10.1109/TIE.2016.2625238.
[29] A.-R. Youssef, E. E. M. Mohamed, and A. I. M. Ali, "Model predictive control for grid-tie wind-energy conversion system based PMSG," in *2018 International Conference on Innovative Trends in Computer Engineering (ITCE)*, Feb. 2018, pp. 467–472, doi: 10.1109/ITCE.2018.8316668.
[30] E. G. Shehata, "A comparative study of current control schemes for a direct-driven PMSG wind energy generation system," *Electric Power Systems Research*, vol. 143, pp. 197–205, Feb. 2017, doi: 10.1016/j.epsr.2016.10.039.
[31] E. J. Fuentes, C. Silva, D. E. Quevedo, and E. I. Silva, "Predictive speed control of a synchronous permanent magnet motor," in *2009 IEEE International Conference on Industrial Technology*, Feb. 2009, pp. 1–6, doi: 10.1109/ICIT.2009.4939731.
[32] E. J. Fuentes, C. A. Silva, and J. I. Yuz, "Predictive speed control of a two-mass system driven by a permanent magnet synchronous motor," *IEEE Transactions on Industrial Electronics*, vol. 59, no. 7, pp. 2840–2848, Jul. 2012, doi: 10.1109/TIE.2011.2158767.
[33] M. Preindl and S. Bolognani, "Model predictive direct speed control with finite control set of PMSM drive systems," *IEEE Transactions on Power Electronics*, vol. 28, no. 2, pp. 1007–1015, Feb. 2013, doi: 10.1109/TPEL.2012.2204277.
[34] J. Gao and J. Liu, "A novel FCS model predictive speed control strategy for IPMSM drives in electric vehicles," in *IECON 2019 - 45th Annual Conference of the IEEE Industrial Electronics Society*, Oct. 2019, pp. 3169–3173, doi: 10.1109/IECON.2019.8927788.
[35] A. Formentini, A. Trentin, M. Marchesoni, P. Zanchetta, and P. Wheeler, "Speed finite control set model predictive control of a PMSM fed by matrix converter," *IEEE Transactions on Industrial Electronics*, vol. 62, no. 11, pp. 6786–6796, Nov. 2015, doi: 10.1109/TIE.2015.2442526.
[36] M. Abdelrahem, C. Hackl, R. Kennel, and J. Rodriguez, "Sensorless predictive speed control of permanent-magnet synchronous generators in wind turbine applications," in *PCIM Europe 2019; International Exhibition and Conference for Power Electronics, Intelligent Motion, Renewable Energy and Energy Management*, 2019, pp. 1–8.
[37] B. Wu, Y. Lang, N. Zargari, and S. Kouro, *Power conversion and control of wind energy systems*. Hoboken, NJ, USA, 2011.
[38] S. Kouro, M. A. Perez, J. Rodriguez, A. M. Llor, and H. A. Young, "Model predictive control: MPC's role in the evolution of power electronics," *IEEE Industrial Electronics Magazine*, vol. 9, no. 4, pp. 8–21, Dec. 2015, doi: 10.1109/MIE.2015.2478920.

BIOGRAPHIES OF AUTHORS

Mai N. Abu Hashish is an M.Sc. Student and demonstrator in the Electrical Engineering Department, Faculty of Engineering, Port Said University, Egypt. She received her B.Sc. degree in Electrical Engineering from Port Said University in 2016. Her research interests are renewable energy systems and model predictive control of power converters.

Ahmed Ali Daoud is an Associate Professor in EE Department at Port Said University, Egypt. His research interests are renewable energy, network analysis, power system stability, demand-side management, and smart grid applications. He is the CEO of the Egyptian Engineering Association, Port Said Branch. He is currently working on a research project involving microgrids incorporating renewable resources and EVs to enhance grid energy management and control. He can be contacted at email: a.daoud@psu.edu.eg or ahmed.ali.daoud@gmail.com.

Medhat Hegazy Elfar is an assistant professor in the Electrical Engineering Department, Faculty of Engineering, Port Said University. He received his Ph.D. degree in Electrical Engineering in 2010, from Port Said University. Since then, he has been an assistant professor at the Electrical Engineering Department, Faculty of Engineering, Port Said University. From June 2014-Dec. 2014, he was a post-doctoral researcher with Energy Research Center, UOIT University, Canada. His current research interests include power electronics and artificial intelligence applications on electrical machines and renewable energy systems. He can be contacted at email: medhat.elfar@gmail.com or mhelfar@hotmail.com.